



## Full Length Article

## Influence of dimethyl ether addition on the oxidation of acetylene in the absence and presence of NO

Lorena Marrodán, Laura Berdusán, Verónica Aranda, Ángela Millera, Rafael Bilbao, María U. Alzueta<sup>\*</sup>

Aragón Institute of Engineering Research (I3A), Department of Chemical and Environmental Engineering, University of Zaragoza, C/ Mariano Esquillor, S/N, 50018 Zaragoza, Spain

## HIGHLIGHTS

- Experimental and modeling study of the C<sub>2</sub>H<sub>2</sub>-DME mixtures oxidation.
- For fuel-rich conditions, DME presence in the mixtures delays C<sub>2</sub>H<sub>2</sub> consumption.
- For fuel-lean conditions, DME presence in the mixtures promotes C<sub>2</sub>H<sub>2</sub> consumption.
- An effective NO diminution could be achieved depending on the oxygen availability.
- Competition between HCCO + NO and HCCO + O<sub>2</sub> determines the final NO diminution.

## ARTICLE INFO

## Article history:

Received 5 March 2016

Received in revised form 20 May 2016

Accepted 2 June 2016

## Keywords:

Dimethyl ether  
C<sub>2</sub>H<sub>2</sub>-DME mixtures  
Oxidation  
Nitrogen oxides

## ABSTRACT

Dimethyl ether (DME) is a promising diesel fuel additive for reducing soot and NO<sub>x</sub> emissions, because of its interesting properties and the possibility of a renewable production. An experimental and modeling study of the oxidation of acetylene (C<sub>2</sub>H<sub>2</sub>, considered as an important soot precursor) and DME mixtures has been performed under well-controlled flow reactor conditions. The influence of temperature, air excess ratio ( $\lambda$ ) and presence of NO on the oxidation process has been analyzed. Under fuel-rich conditions, the presence of DME in these mixtures modifies the radical pool delaying the acetylene consumption. C<sub>2</sub>H<sub>2</sub> and DME, and the radicals generated in their conversion, interact with NO achieving different levels of NO concentration diminution depending upon the operating conditions. Under fuel-lean conditions, the presence of DME in the mixtures increases the NO diminution, whereas for the other values of  $\lambda$  considered, the maximum NO decrease reached is lower than that obtained in the case of pure acetylene.

© 2016 Published by Elsevier Ltd.

## 1. Introduction

The use of oxygenated compounds as additives to diesel fuels is considered nowadays as a promising alternative for minimizing soot emissions and maybe also NO<sub>x</sub> under appropriate conditions [1,2]. Classical oxygenated compounds include alcohols and ethers, and among them, ethanol (C<sub>2</sub>H<sub>5</sub>OH) and dimethyl ether (CH<sub>3</sub>OCH<sub>3</sub>, DME) are two of the most popular candidates to be used as additives. The use of ethanol has been extensively studied in the last years and it is already being used in reformulated gasolines, like E85 (85% ethanol and 15% gasoline) [3]. Similarly, DME has received considerable attention because of its high cetane number, vaporization characteristics, low toxicity, and low tendency to produce smoke and volatile organic compounds (VOCs) [4]. Additionally, DME can be produced from renewable materials [5,6].

Ethanol and DME have the same molecular formula (C<sub>2</sub>H<sub>6</sub>O) but different structure and functional group, and, as it has been discussed in several previous works (e.g. [7,8]), the oxygen content and the specific structure of the oxygenated compound strongly influence the capacity for pollutant emission minimization. Song et al. [9] concluded that, under the conditions of their modeling study, both DME and ethanol were effective in reducing aromatic species (important soot precursors). However, DME exhibited a greater effectiveness due to its higher enthalpy of formation, which led to a higher final flame temperature and consequently to a decrease in aromatic species production in premixed flames [10], but also because of its structure. For fuel-rich conditions, the reaction flux analysis conducted by these authors [9] determined that reactions involving DME convert only approximately 15% of its carbon to C<sub>2</sub>-species (key species in the production of aromatic species), whereas reactions of ethanol convert approximately 35% of its carbon to C<sub>2</sub>-species.

In previous works of our group, focused on the formation of soot (e.g. [11–13]), acetylene was selected as fuel because it is

<sup>\*</sup> Corresponding author.E-mail address: [uxue@unizar.es](mailto:uxue@unizar.es) (M.U. Alzueta).

recognized as an important soot precursor [14,15]. Furthermore, to analyze the influence of the addition of oxygenated compounds on the reduction of soot emissions, pyrolysis experiments of acetylene-ethanol mixtures were performed [16]. Results indicated that increasing the amount of ethanol in the mixture leads to a diminution on the soot production compared to the acetylene case. The influence of the oxygenated structure was also analyzed by considering the sooting tendency of two isomers, ethanol and DME [17], and the origin of both carbon and, in particular, oxygen appears to be critical for the formation of soot. DME has no C–C bonds and this fact can be the reason for DME to produce less soot than ethanol.

The performance, suitability and proper diesel engine operation of diesel-DME blends have already been reported in different works [18,19]. Therefore, taking into account these promising results, studies under well-controlled laboratory conditions may help to understand the influence of DME addition on the behavior of soot precursors in the overall oxidation process.

In this context, the present work aims to achieve a better knowledge of the  $C_2H_2$ -DME mixtures oxidation, as well as of the interaction of these mixtures with NO. A parametric study of the conversion of  $C_2H_2$ -DME mixtures has been done, analyzing the influence of temperature, air excess ratio and DME concentration in these mixtures. Experiments have been performed both in the absence and presence of NO, thus allowing to determine both the impact of the NO presence on the oxidation regime of the mixtures and the capability of these mixtures to reduce NO. The experimental results have been interpreted in terms of a detailed kinetic mechanism built up from different individual reaction subsets taken from literature.

## 2. Experimental

Oxidation experiments of  $C_2H_2$ -DME mixtures, both in the absence and presence of NO, have been carried out in a gas-phase installation at atmospheric pressure, which has been described in detail elsewhere (e.g. [7]) and, therefore, only a brief description is given here.

Gases are fed to the system from gas cylinders through mass flow controllers in four separate streams: a main flow containing  $N_2$  and water vapor (fed by saturating a  $N_2$  stream through a water bubbler), and three injector tubes for the reactants ( $C_2H_2$ , DME,  $O_2$  and NO).  $N_2$  is used to balance, to obtain a total flow rate of 1000 mL(STP)/min. The injection system has been configured following the investigations of Alzueta et al. [20].

The experiments have been carried out at atmospheric pressure, in the 575–1475 K temperature range and for different values of the air excess ratio ( $\lambda$ ), ranging from fuel-rich ( $\lambda = 0.2$ ) to fuel-lean ( $\lambda = 20$ ) conditions. The air excess ratio is defined as the inlet oxygen concentration divided by the stoichiometric oxygen. Approximately, 500 ppm of  $C_2H_2$  and 5000 ppm of water vapor were introduced in all the experiments, whereas for DME, two different amounts, 50 and 200 ppm, have been used. Table 1 lists the conditions of the different experiments.

Reaction takes place in a quartz plug flow reactor, following the design of Kristensen et al. [21], which has a reaction zone of 8.7 mm inside diameter and 200 mm in length. The reactor is placed in a three-zone electrically heated furnace, ensuring a uniform temperature profile throughout the reaction zone within  $\pm 10$  K. The temperature in the reaction zone is measured with a type K fine-wire thermocouple placed into a thin tube along the reactor without contact with gases. The total flow rate (1000 mL (STP)/min) is kept constant during the experiments leading to different gas residence times ( $t_r$ : 340–132 ms) depending on the temperature in the isothermal reaction zone, being  $t_r$  (s) = 195/T(K).

**Table 1**

Matrix of experimental conditions. The experiments are conducted at constant flow rate of 1000 mL(STP)/min, in the temperature interval of 575–1475 K. The balance is closed with  $N_2$ .  $t_r$  (s) = 195/T(K).

Set	$\lambda$	$C_2H_2$ (ppm)	DME (ppm)	$O_2$ (ppm)	NO (ppm)	$H_2O$ (ppm)	Source <sup>a</sup>
1	0.2	500	50	280	0	5000	pw
2	0.2	500	200	370	0	5000	pw
3	0.2	500	200	370	500	5000	pw
4	0.2	500	0	250	500	7000	[23]
5	0.7	500	50	980	0	5000	pw
6	0.7	500	200	1295	0	5000	pw
7	0.7	500	200	1295	500	5000	pw
8	0.7	500	0	875	500	7000	[23]
9	0.7	500	0	875	0	7000	[22]
10	1	500	50	1400	0	5000	pw
11	1	500	200	1850	0	5000	pw
12	1	500	200	1850	500	5000	pw
13	1	500	0	1250	500	7000	[23]
14	20	500	50	28,000	0	5000	pw
15	20	500	200	37,000	0	5000	pw
16	20	500	200	37,000	500	5000	pw
17	20	500	0	25,000	500	5000	pw
18	20	500	0	25,000	0	7000	[22]

<sup>a</sup> "pw" denotes present work.

At the end of the reactor, the reaction is efficiently quenched by means of external refrigeration with air. The outlet gas composition is analyzed by a micro-gas chromatograph (Agilent 3000) equipped with TCD detectors. In addition to  $C_2H_2$ , CO,  $CO_2$ , which are the majority gases, other compounds can be detected by chromatography. Among these, only  $H_2$ ,  $CH_4$ ,  $C_2H_6$  and  $C_2H_4$  were detected in appreciable amounts. The DME concentration is measured with an Ati Mattson Fourier transform infrared (FTIR) spectrometer. The NO concentration is measured using a continuous IR analyzer (URAS 26, ABB). The uncertainty of the measurements is estimated as  $\pm 5\%$  but not less than 10 ppm, for both the continuous analyzers and the gas chromatograph.

An atomic carbon balance was performed in the experiments by a comparison of the carbon contained in the product gas and the carbon contained in the reactants fed to the reactor, and in all the experiments was closed within  $100 \pm 10\%$ .

Additional experimental data have been taken from previous works of Alzueta et al. [22] and Abián et al. [23] who, in the same experimental installation, carried out different oxidation experiments of acetylene in the absence and presence of NO, respectively.

## 3. Reaction mechanism

The experimental results have been analyzed in terms of a detailed gas-phase chemical kinetic model. The mechanism used as starting point for the modeling study is that previously developed by our group for the oxidation of acetylene-ethanol mixtures in the absence and presence of NO [7]. The initial mechanism included the reactions to describe interactions between  $C_1$ - $C_2$  hydrocarbons and NO by Glarborg et al. [24,25], reactions for acetylene conversion by Alzueta et al. [22], and reactions for ethanol oxidation by Alzueta and Hernández [26].

In the present work, the DME reaction subset proposed by Alzueta et al. [27] has been added to the initial mechanism. Moreover, a reaction subset for glyoxal (OCHCHO) oxidation [28] has also been included, because this species is recognized as an important intermediate in hydrocarbons combustion and, at low to medium temperatures, it can be formed during the  $C_2H_2$  oxidation through the sequence:  $C_2H_2 \xrightarrow{+OH} C_2H_2OH \xrightarrow{+O_2} OCHCHO + OH$ . In the starting mechanism [7], only one global reaction involving glyoxal decomposition was taken into account.

The full reaction mechanism includes 100 species and 613 reactions. Thermodynamic data for the involved species have been taken from the same sources as the origin mechanisms. The most important reactions are discussed below, and the final updated mechanism is provided as Supplementary material. The Chemkin version can be obtained directly from the authors.

Calculations have been performed using the Senkin code [29], the plug flow reactor code that runs in conjunction with the Chemkin-II library [30], considering constant pressure and temperature in the reaction zone.

#### 4. Results and discussion

A study of the oxidation of  $C_2H_2$ -DME mixtures at atmospheric pressure in the 575–1475 K temperature range has been performed. The influence of temperature, air excess ratio ( $\lambda$ ), amount of DME present in the mixture and the presence of NO on the conversion of these mixtures has been analyzed. The study of the influence of these variables has been done by analyzing the outlet concentration of the majority carbon species ( $C_2H_2$ , DME, CO and  $CO_2$ ) and NO. Other species ( $CH_4$ ,  $C_2H_6$  and  $C_2H_4$ ) have also been detected but in very small amounts and, therefore, their results are not shown.

##### 4.1. $C_2H_2$ -DME mixtures oxidation in the absence of NO

The air excess ratio ( $\lambda$ ) has been varied from fuel-rich ( $\lambda = 0.2$ ) to fuel-lean conditions ( $\lambda = 20$ ), keeping constant the concentration of  $C_2H_2$  (500 ppm) and DME (200 ppm) and the results obtained (corresponding to sets 2, 6, 11 and 15 in Table 1) have been compared. Similar results (not shown) have been obtained for 50 ppm of DME (sets 1, 5, 10 and 14 in Table 1).

Fig. 1 shows the influence of the temperature and air excess ratio on the concentration of DME,  $C_2H_2$ , CO and  $CO_2$ . For CO and  $CO_2$ , the carbon yield has been defined as the  $CO_{outlet}/2[C_2H_2 + DME]_{inlet}$  and  $CO_{outlet}/2[C_2H_2 + DME]_{inlet}$  ratios. In general, the

used model provides good agreement between experimental results and modeling calculations, reproducing well the main experimental trends observed. However, certain discrepancies are observed, especially for acetylene. This can be due to the fact that the model exclusively includes gas-phase reactions; it does not consider PAH and soot formation pathways involving  $C_2H_2$  according to HACA route [14], which may be important under given conditions, such as the very fuel-rich conditions ( $\lambda = 0.2$ ) of this work.

As it can be observed in Fig. 1, the onset temperature for  $C_2H_2$  and DME conversion depends on the oxygen availability. This temperature increases as the value of  $\lambda$  decreases, being quite similar for fuel-rich ( $\lambda = 0.7$ ) and very fuel-rich conditions ( $\lambda = 0.2$ ) for acetylene, and also for stoichiometric conditions for DME. The results differ from those reported by Alzueta et al. [22] in a study of pure  $C_2H_2$  oxidation, where the onset for the  $C_2H_2$  conversion was approximately the same, independent of the stoichiometry (values of  $\lambda$  up to  $\lambda = 20$ ). Something similar can be said about DME. In the DME oxidation work by Alzueta et al. [27], the oxygen availability had a slightly influence on the onset of pure DME oxidation. Thus, the results of the present work indicate an effective interaction of the compounds and/or their derivatives in the mixtures.

At the highest temperatures considered, DME is completely consumed for all the  $\lambda$  values studied, even under reducing conditions, because it mainly decomposes thermally above a given temperature, as it is later discussed. Alzueta et al. [27] stated that DME oxidation does not take place or proceeds very slowly at temperatures lower than 1000 K, and this is the behavior observed for the different air excess ratios analyzed, except for  $\lambda = 20$ , where DME conversion starts at lower temperatures, approximately 100 K less. On the other hand, acetylene is not always completely consumed. For  $\lambda = 0.2$ , when the oxygen availability is lower, and at the highest temperatures reached, about 250 ppm of  $C_2H_2$  still remain unconverted, which is also predicted by the model. Once DME is completely consumed,  $C_2H_2$  shows a steeper decay. Moreover, at the fuel leanest conditions studied ( $\lambda = 20$ ), the full conversion of

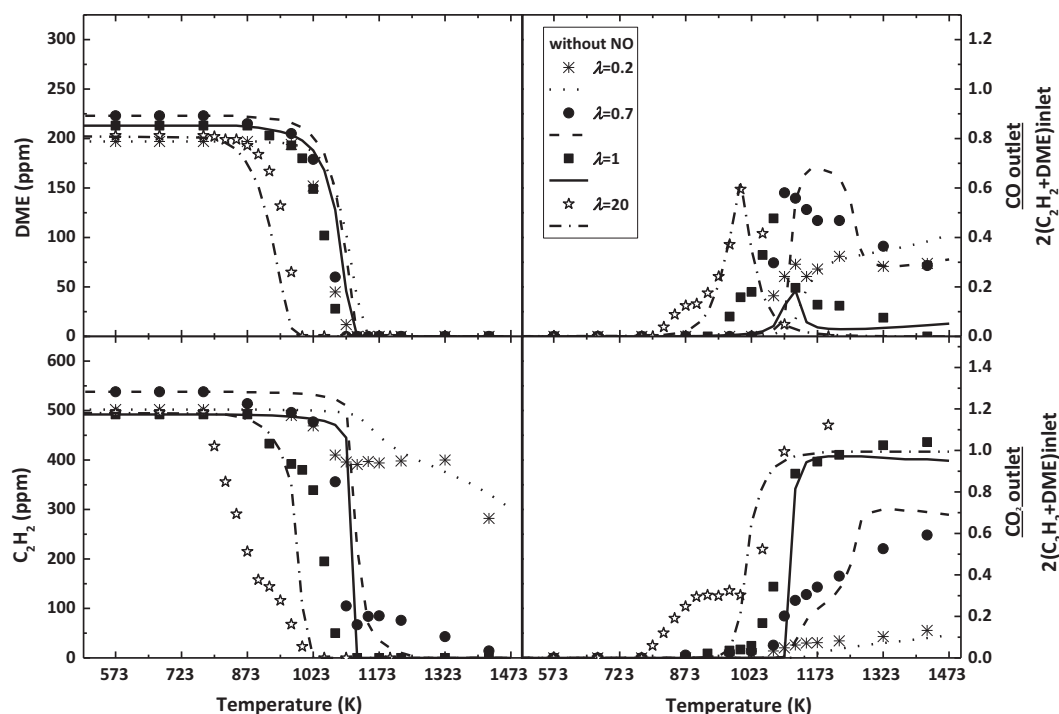


Fig. 1. Concentrations of DME and  $C_2H_2$ , and  $CO_{outlet}/2[C_2H_2 + DME]_{inlet}$  and  $CO_{outlet}/2[C_2H_2 + DME]_{inlet}$  ratios as a function of the temperature for different air excess ratios. Comparison between experimental (symbols) and modeling results (lines) (sets 2, 6, 11 and 15 in Table 1).

acetylene occurs approximately at 75 K below compared to stoichiometric conditions. Obviously, what is seen for  $\lambda = 20$  is reflected in the CO and CO<sub>2</sub> experimental concentration profiles, which start to be formed as C<sub>2</sub>H<sub>2</sub> starts to be consumed. The CO concentration reaches a maximum, and the CO<sub>2</sub> concentration continuously increases reaching a higher value as the conditions become fuel leaner. This is attributed to the fact that after the initiation of the acetylene conversion, mainly by its reaction with O<sub>2</sub> forming formyl radical (HCO) (reaction (R.1)), the main consumption of acetylene occurs through the interaction with O radicals (reaction (R.2)) generating HCCO species. Afterwards, both HCO and HCCO give CO and subsequently CO<sub>2</sub> (reactions (R.3)–(R.6)).



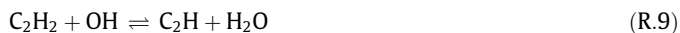
The availability of oxygen affects the temperature at which CO peaks. As the mixture becomes fuel leaner, the CO peak is shifted to lower temperatures and becomes sharper, except for  $\lambda = 0.2$ , for which the CO concentration increases in all the temperature range studied.

Reaction rate analyses for the oxidation of different C<sub>2</sub>H<sub>2</sub>-DME mixtures have been performed to identify the reactions that contribute to the C<sub>2</sub>H<sub>2</sub> and DME consumption. The results indicate that the main routes for C<sub>2</sub>H<sub>2</sub> consumption are similar to those reported by Alzueta et al. [22] for the individual C<sub>2</sub>H<sub>2</sub> conversion and that the DME reaction pathways hardly differ from those described by Alzueta et al. [27], even though the presence of certain radicals (e.g. OH radicals) may increase the relevance of some of these routes as described below.

The initiation reactions for C<sub>2</sub>H<sub>2</sub> conversion include its interaction with O<sub>2</sub> (reaction (R.1)) and the H, O and OH radicals. The addition of H to C<sub>2</sub>H<sub>2</sub> to form vinyl radicals (reaction (R.7)) appears to be an important C<sub>2</sub>H<sub>2</sub> consumption reaction, especially for  $\lambda = 0.2$ , 0.7 and 1.

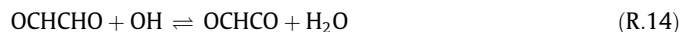
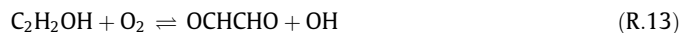
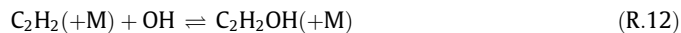


This reaction is in competition with others involving interactions of C<sub>2</sub>H<sub>2</sub> with O radicals (reactions (R.2) and (R.8)) and also with OH radicals, but with a minor relevance (reactions (R.9)–(R.11)).

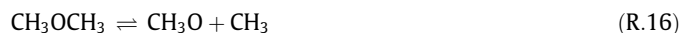


Under fuel-lean conditions, the C<sub>2</sub>H<sub>2</sub> interaction with OH radicals to form C<sub>2</sub>H<sub>2</sub>OH gains relevance (reaction (R.12)). For example, at 873 K, the net rate of production of C<sub>2</sub>H<sub>2</sub>OH through reaction (R.12) increases from  $1.00 \times 10^{-15}$  mol/cm<sup>3</sup> s, for  $\lambda = 0.2$ , to  $1.00 \times 10^{-11}$  mol/cm<sup>3</sup> s, for  $\lambda = 20$ . The generated species are involved in reactions with oxygen molecular to form glyoxal (OCHCHO, reaction (R.13)), which seems to be an important intermediate in combustion of hydrocarbons as it can be formed from C<sub>2</sub>H<sub>2</sub>

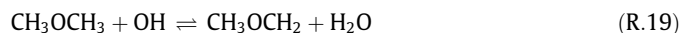
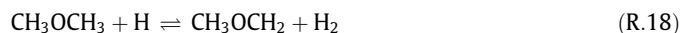
oxidation [28]. Glyoxal reacts with OH radicals to form OCHCO (reaction (R.14)), which finally decomposes to formyl radicals and CO (reaction (R.15)).



On the other hand, the conversion of DME is mainly initiated by its unimolecular decomposition:



Other important consumption reactions include hydrogen abstraction of DME by the radical pool (reactions (R.17)–(R.19)) and interaction of DME with CH<sub>3</sub> radicals (reaction (R.20)) to produce CH<sub>3</sub>OCH<sub>2</sub> radicals, which decompose to obtain formaldehyde (reaction (R.21)), that follows the CH<sub>2</sub>O → HCO → CO → CO<sub>2</sub> reaction sequence.



To evaluate the influence of the DME amount present in the mixture on the C<sub>2</sub>H<sub>2</sub> and DME consumption, in Fig. 2, the results obtained for the experiments performed under fuel-rich ( $\lambda = 0.7$ ) and fuel-lean ( $\lambda = 20$ ) conditions for two different inlet DME amounts (50 and 200 ppm) have been compared (sets 5, 6, 9, 14, 15 and 18 in Table 1). From a previous work of our group [22], results of the C<sub>2</sub>H<sub>2</sub> oxidation without DME have been taken as reference. For stoichiometric conditions, similar results (not shown) as those for  $\lambda = 0.7$  have been obtained.

The temperature for the onset of the DME conversion is almost independent of the amount present in the mixture (50 or 200 ppm), although for  $\lambda = 0.7$  DME is consumed completely at lower temperatures, approximately 75 K less in the experiments, for the DME lowest amount considered.

The DME presence in the mixture has a different impact whether the ambient is fuel-rich or fuel-lean. Whereas for  $\lambda = 0.7$ , increasing the amount of DME seems to have an inhibiting effect on acetylene consumption, for  $\lambda = 20$ , the presence of DME shifts the C<sub>2</sub>H<sub>2</sub> concentration profiles towards lower temperatures.

Reaction rate analyses have been performed to elucidate this fact. As mentioned before, the main C<sub>2</sub>H<sub>2</sub> conversion occurs through its reactions with O<sub>2</sub> (reaction (R.1)) and O and OH radicals (reactions (R.2), (R.8)–(R.11)), but for fuel-rich conditions, reaction (R.7), that involves H addition to form vinyl radicals, becomes a really important C<sub>2</sub>H<sub>2</sub> consumption reaction. When DME is present in the mixture, some of these H radicals are then involved in DME consumption (reaction (R.18), DME + H ⇌ CH<sub>3</sub>OCH<sub>2</sub> + H<sub>2</sub>). For example, at 1023 K, when DME is not present in the mixture, H radical consumption by reaction (R.7) (C<sub>2</sub>H<sub>2</sub> + H(±M) ⇌ C<sub>2</sub>H<sub>3</sub>(±M)) is approximately 34%; when 50 ppm of DME are present in the mixture, this value decreases to 29% (a 33% of H radical consumption is by reaction (R.18)); and, when the amount of DME is increased to 200 ppm, only a 13% of H radicals is consumed by reaction (R.7) (and a 68% by reaction (R.18)). As a result, less H radicals participate in C<sub>2</sub>H<sub>2</sub> consumption, and its conversion is shifted

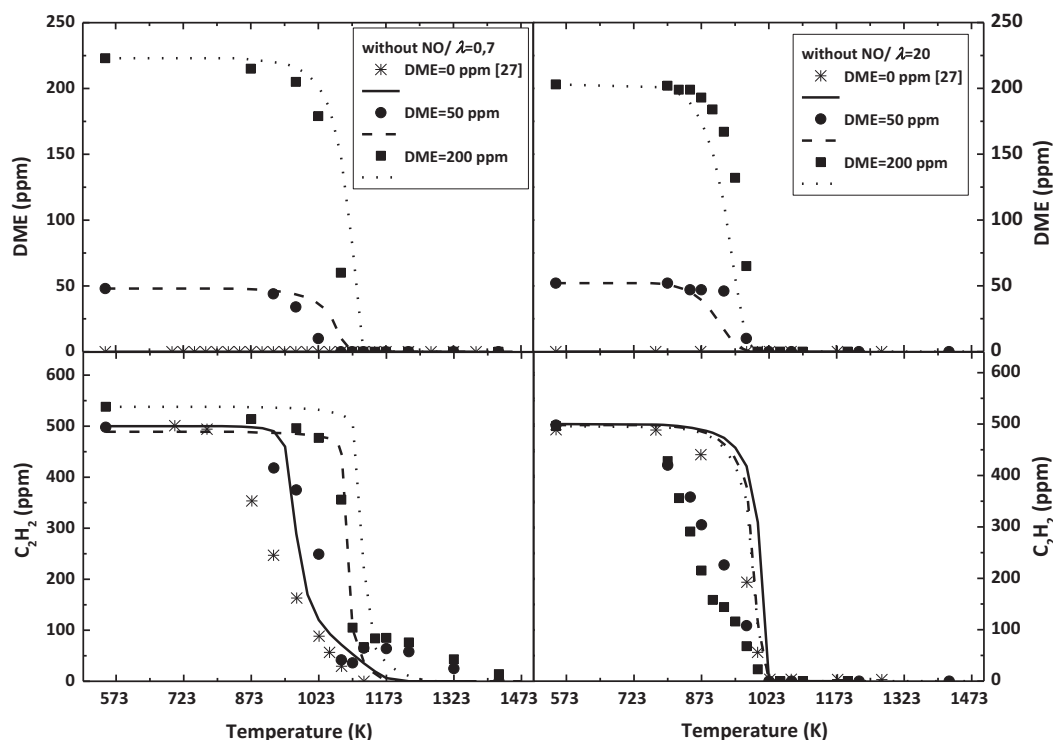


**Fig. 2.** Concentrations of DME and C<sub>2</sub>H<sub>2</sub> as a function of the temperature depending on the DME inlet concentration for  $\lambda = 0.7$  (left) and  $\lambda = 20$  (right). Comparison between experimental (symbols) and modeling results (lines) (sets 5, 6, 9, 14, 15 and 18 in Table 1).

to higher temperatures when DME is present in the mixture (the higher the DME amount, the higher C<sub>2</sub>H<sub>2</sub> conversion temperatures).

On the other hand, when the oxygen availability is increased ( $\lambda = 20$ , right in Fig. 2), the conversion of both DME and acetylene occurs at lower temperatures than for fuel-rich conditions, and the presence of DME in the reactant mixture promotes C<sub>2</sub>H<sub>2</sub> conversion (there is not a big difference in adding 50 or 200 ppm of DME to the reactant mixture), although it can only be observed experimentally. One probable explanation could be that the presence of DME in the mixture entails a greater amount of oxygen that can react with both C<sub>2</sub>H<sub>2</sub> and DME. The formation of OH radicals is enlarged because of the increase in the available oxygen and DME is mainly consumed by its reaction with OH (reaction (R.19)). Acetylene reacts with O<sub>2</sub> too (reaction (R.1)), but also with O and OH radicals (reactions (R.2) and (R.8)–(R.11)), which formation is increased because of the fuel-leaner conditions. As a result, both DME and C<sub>2</sub>H<sub>2</sub> conversions are shifted to lower temperatures than for fuel-rich conditions. However, at present, the model fails to reproduce the C<sub>2</sub>H<sub>2</sub> profile, probably due to uncertainties in the mechanism describing C<sub>2</sub>H<sub>2</sub> conversion.

#### 4.2. C<sub>2</sub>H<sub>2</sub>-DME mixtures oxidation in the presence of NO

Although some authors indicate that NO<sub>x</sub> emissions when DME is used as fuel are higher or of a similar level than with diesel fuel in a compression ignition engine at the same operating conditions (e.g. [31]), others indicate that when operating under optimized conditions (such as changing the injection system), NO<sub>x</sub> emissions from DME are lower than from diesel [32]. Those studies correspond to experiments in real engines, and may be significantly different or involve many different parameters affecting the global results. Thus, studies carried out under well-controlled conditions may be helpful to understand how the DME-NO interaction proceeds. Therefore, oxidation experiments of C<sub>2</sub>H<sub>2</sub>-DME mixtures in

the presence of NO, for different air excess ratios, have also been carried out (Table 1).

NO may interact with C<sub>2</sub>H<sub>2</sub>, DME and their derivatives, achieving some degree of diminution depending on the conditions. Under fuel-rich conditions, NO could be decreased by reburn reactions by reacting with hydrocarbon radicals produced during the oxidation of DME and C<sub>2</sub>H<sub>2</sub> [20,33–35]. Under fuel-lean conditions, NO may favor the oxidation of the C<sub>2</sub>H<sub>2</sub>-DME mixture in a mutually sensitized oxidation process, similar to what has been observed for other compounds such as methane [36], ethanol and methanol [37].

To elucidate the impact of the DME presence in the C<sub>2</sub>H<sub>2</sub>-DME mixtures for NO diminution, the present experimental results have been compared (Fig. 3) with those of Abián et al. [23] for the interaction between C<sub>2</sub>H<sub>2</sub> and NO for different air excess ratios

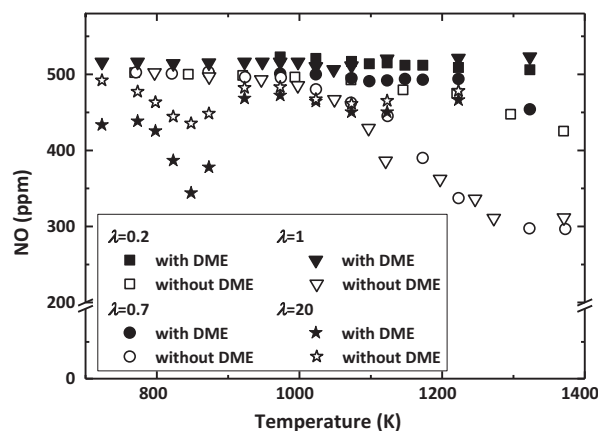


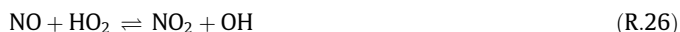
**Fig. 3.** Experimental results for NO concentration as a function of the temperature for different air excess ratios in the presence (solid symbols) and absence (empty symbols) [23] of DME (sets 3, 4, 7, 8, 12, 13, 16 and 17 in Table 1).



(corresponding to sets 4, 8 and 13 in Table 1). To complete that work, an experiment under similar conditions, but for  $\lambda = 20$ , has been performed in the present work (set 17 in Table 1).

When no DME is present in the mixture, at temperatures higher than 1300 K and for  $\lambda = 0.7$  and 1, the NO amount decreases from 500 ppm to about 300 ppm, which means a 40% diminution in NO. This represents the highest NO decrease percentage achieved under the conditions of this work, because for  $\lambda = 0.2$  only a 15% and for  $\lambda = 20$  a 13% (at lower temperatures) decrease in NO were respectively obtained. When DME is present in the mixture, it has its main effect under fuel-lean conditions, when the NO decrease percentage rises from 13% up to 30%.

Consistent with modeling predictions, and in concordance with literature [22,23], acetylene is an important source of HCCO radicals ( $\text{C}_2\text{H}_2 + \text{O} \Rightarrow \text{HCCO} + \text{H}$ , reaction (R.2)). These radicals can be involved in the NO concentration diminution. For fuel-rich conditions, HCCO radicals interact with NO (reactions (R.22) and (R.23)) explaining the NO experimental decrease of 40% for  $\lambda = 0.7$  and 1, and 15% for  $\lambda = 0.2$ , at 1300 K, in the absence of DME. However, by increasing the oxygen concentration ( $\lambda = 20$ ), the HCCO + NO reactions are less important and the HCCO +  $\text{O}_2$  reactions (reactions (R.24) and (R.25)) predominate. Due to this fact, for  $\lambda = 20$ , when no DME is added, the NO diminution occurs only by conversion to  $\text{NO}_2$  (reaction (R.26)), resulting in a lower NO lessening achieved. Thus, the competition between these two HCCO radicals consumption steps (with NO or  $\text{O}_2$ ) determines the final level of NO lessening achieved.



Under fuel-lean conditions, the DME addition causes an increase in the NO diminution (experimentally from a 13% up to 30%) due to its interaction with  $\text{CH}_3$  radicals (which are generated by DME decomposition, reaction (R.16)) by reactions (R.27) and (R.28).



To deeply analyze the influence of the NO presence on the oxidation of the  $\text{C}_2\text{H}_2$ -DME mixtures, the DME and  $\text{C}_2\text{H}_2$  experimental results and calculations (Fig. 4) can be compared with those earlier represented in Fig. 1 (under similar experimental conditions but in the absence of NO). Calculations predict reasonably well the trends obtained, with the exception of NO conversion under fuel-rich conditions, which is overestimated.

The presence of NO has its major effect under fuel-lean conditions, causing both  $\text{C}_2\text{H}_2$  and DME concentration profiles to shift to lower temperatures; a shift of more than 200 K in the temperature for the onset of DME oxidation, similar to that observed by Alzueta et al. [27] in the study of pure DME oxidation in the presence of NO.

Reaction rate analyses performed indicate that the main routes for  $\text{C}_2\text{H}_2$  and DME conversion, already described in the absence of NO, are mostly the same than those obtained in the presence of NO for the conditions studied in this work. In the initial steps of  $\text{C}_2\text{H}_2$  conversion (approximately 850–875 K), the reaction of  $\text{C}_2\text{H}_2$  with OH (reaction (R.12)), important under oxidizing conditions, becomes even more relevant in presence of NO. It represents the

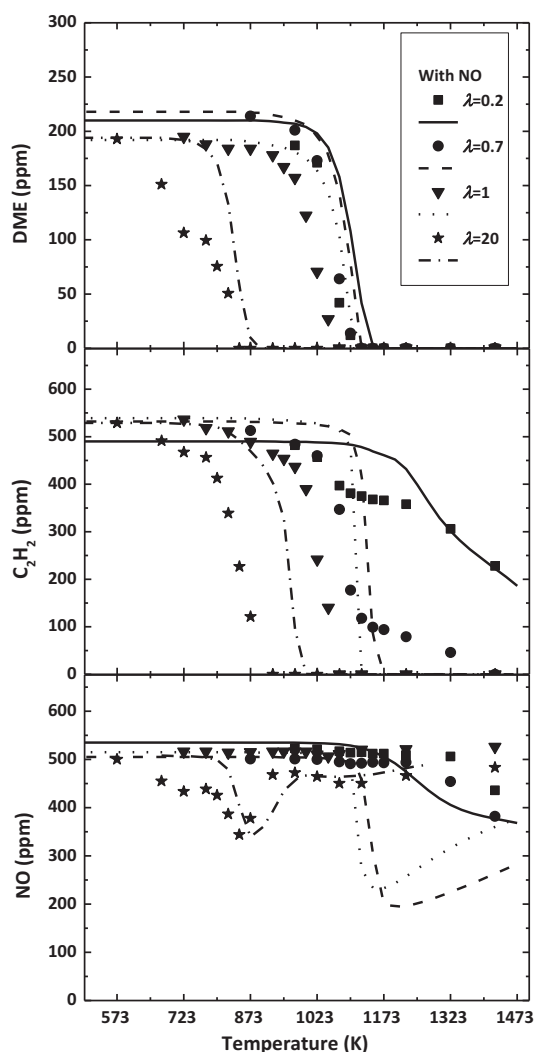
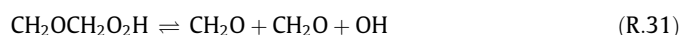
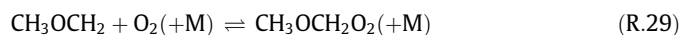


Fig. 4. Concentrations of DME,  $\text{C}_2\text{H}_2$  and NO as a function of temperature for different air excess ratios. Comparison between experimental (symbols) and modeling results (lines) (sets 3, 7, 12 and 16 in Table 1).

first step in the formation of glyoxal (reaction (R.13)), an important intermediate under these conditions. The presence of NO also enhances reactions of acetylene consumption and HCCO and  $\text{CH}_2$  radicals generation (reactions (R.2) and (R.8), respectively). As a result, the  $\text{C}_2\text{H}_2$  oxidation in the presence of NO becomes faster under oxidizing conditions.

For  $\lambda = 20$  and in the presence of NO, the main reaction routes for DME change slightly. The main consumption of DME is by interaction with OH radicals through reaction (R.19) (i.e.  $\text{CH}_3\text{OCH}_3 + \text{OH} \Rightarrow \text{CH}_3\text{OCH}_2 + \text{H}_2\text{O}$ ). The DME radicals ( $\text{CH}_3\text{OCH}_2$ ) generated react with  $\text{O}_2$  forming peroxy species, which continue reacting until formaldehyde is obtained (reactions (R.29)–(R.31)). Alzueta et al. [27] stated that, at temperatures lower than 900 K, the DME oxidation route through methoxymethyl-peroxy ( $\text{CH}_3\text{OCH}_2\text{O}_2$ ) may be important, similarly to that observed in the oxidation of dimethoxymethane ( $\text{CH}_3\text{OCH}_2\text{OCH}_3$ ) under oxidizing conditions and increasing pressure [38].



**Table 2**Linear sensitivity coefficients for CO for the selected sets<sup>a</sup>.

Reaction	Set 2 1073 K	Set 3 1073 K	Set 6 1023 K	Set 7 1023 K	Set 10 973 K	Set 11 998 K	Set 12 998 K	Set 15 848 K	Set 16 798 K
$C_2H_2 + O_2 \rightleftharpoons HCO + HCO$	0.433	0.402	0.929	0.930	1.128	1.001	1.023	1.056	1.714
$C_2H_2 + O \rightleftharpoons HCCO + H$	0.018	−0.004	0.025	0.003	0.060	0.029	0.008	0.025	0.053
$C_2H_2 + H(+M) \rightleftharpoons C_2H_3(+M)$	0.011	0.009	0.039	0.039	0.114	0.047	0.057	0.013	0.037
$C_2H_2OH + O_2 \rightleftharpoons OCHCHO + OH$	–	–	–	–	–	–	–	0.005	0.056
$OCHCHO + OH \rightleftharpoons OCHCO + H_2O$	–	–	–	–	–	–	–	0.002	0.066
$C_2H_3 + O_2 \rightleftharpoons CH_2O + HCO$	0.072	0.081	0.038	0.055	0.055	0.024	0.042	−0.001	−0.008
$CH_3 + CH_3(+M) \rightleftharpoons C_2H_6(+M)$	−0.185	−0.212	−0.063	−0.074	−0.084	−0.049	−0.063	−0.104	−0.256
$CH_3 + HO_2 \rightleftharpoons CH_3O + OH$	0.007	–	0.021	–	0.183	0.037	–	0.286	0.001
$CH_4 + OH \rightleftharpoons CH_3 + H_2O$	0.057	0.055	0.015	0.015	0.019	0.011	0.013	0.000	0.001
$CH_2O + OH \rightleftharpoons HCO + H_2O$	0.053	0.063	0.033	0.041	0.126	0.035	0.054	0.051	0.541
$CH_2O + H \rightleftharpoons HCO + H_2$	0.137	0.154	0.032	0.038	0.020	0.021	0.030	0.001	0.003
$CH_2O + CH_3 \rightleftharpoons HCO + CH_4$	0.387	0.405	0.107	0.112	0.046	0.067	0.076	0.005	0.009
$HCO + M \rightleftharpoons H + CO + M$	−0.006	−0.012	−0.007	−0.035	0.068	0.001	−0.043	0.037	0.017
$HCO + O_2 \rightleftharpoons CO + HO_2$	0.006	0.009	0.007	0.017	−0.067	−0.001	0.021	−0.038	0.035
$HCCO + O_2 \rightleftharpoons CO + CO + OH$	0.007	0.004	0.007	0.012	−0.003	0.007	0.016	0.007	0.010
$CH_3OCH_3 \rightleftharpoons CH_3O + CH_3$	0.839	0.861	0.167	0.170	0.024	0.073	0.071	–	–
$CH_3OCH_3 + H \rightleftharpoons CH_3OCH_2 + H_2$	−0.348	−0.313	−0.304	−0.304	−0.479	−0.295	−0.353	−0.008	−0.008
$CH_3OCH_3 + O \rightleftharpoons CH_3OC + H_2 + OH$	−0.012	−0.003	−0.021	−0.011	−0.016	−0.026	−0.014	−0.017	0.023
$CH_3OCH_3 + OH \rightleftharpoons CH_3OCH_2 + H_2O$	−0.057	−0.067	−0.041	−0.051	−0.159	−0.043	−0.069	−0.033	0.831
$CH_3OCH_3 + CH_3 \rightleftharpoons CH_3OCH_2 + CH_4$	0.063	0.065	0.024	0.024	0.007	0.016	0.016	0.002	0.000
$CH_3OCH_2 \rightleftharpoons CH_3 + CH_2O$	–	–	–	–	−0.001	–	0.000	−0.026	0.140
$CH_3OCH_3 + O_2(+M) \rightleftharpoons CH_3OCH_2O_2(+M)$	–	–	–	–	–	–	–	0.006	−0.035
$CH_3OCH_2 + O_2 \rightleftharpoons CH_2O + CH_2O + OH$	–	–	–	–	–	–	–	0.007	−0.041
$CH_2OCH_2O_2H \rightleftharpoons CH_2O + CH_2O + OH$	–	–	–	–	–	–	–	0.001	−0.027
$O + OH \rightleftharpoons O_2 + H$	0.110	0.061	0.118	0.077	0.269	0.122	0.093	0.158	0.277
$H + O_2 + N_2 \rightleftharpoons HO_2 + N_2$	0.007	0.010	0.004	0.011	−0.062	0.000	0.014	−0.173	−0.204
$CH_3 + NO \rightleftharpoons HCN + H_2O$	–	−0.011	–	−0.004	–	–	−0.003	–	−0.008
$CH_3 + NO \rightleftharpoons H_2CN + OH$	–	0.072	–	0.033	–	–	0.031	–	0.020
$C_2H_3 + NO \rightleftharpoons C_2H_2 + HNO$	–	0.005	–	0.011	–	–	0.014	–	0.080
$HCO + NO \rightleftharpoons HNO + CO$	–	0.004	–	0.019	–	–	0.024	–	−0.022
$HCCO + NO \rightleftharpoons HCN + CO_2$	–	−0.010	–	−0.017	–	–	−0.021	–	−0.012
$CH_3 + NO_2 \rightleftharpoons CH_3O + NO$	–	0.004	–	0.015	–	–	0.035	–	0.049
$NO_2 + H \rightleftharpoons NO + OH$	–	−0.002	–	−0.007	–	–	−0.015	–	−0.069

<sup>a</sup> The sensitivity coefficients are given as  $A_i \delta Y_j / Y_j \delta A_i$ , where  $A_i$  is the pre-exponential constant for reaction  $i$  and  $Y_j$  is the mass fraction of the  $j$ th species. Therefore, the sensitivity coefficients listed can be interpreted as the relative change in predicted concentration for the species  $j$  caused by increasing the rate constant for reaction  $i$  by a factor of 2.

The interactions between DME and NO, that could produce a NO diminution, were also analyzed by Alzueta et al. [27]. These authors indicated that, under fuel-rich and stoichiometric conditions and temperatures above 1100 K, some NO is reduced and converted into HCN and  $N_2$  by reburn-type reactions with the radicals generated from DME decomposition. However, under fuel-lean conditions and in the 800–1000 K temperature range, a considerable fraction of NO is oxidized to  $NO_2$  (a 20% experimentally and a 40% based on modeling predictions), while no net  $NO_x$  reduction is observed.

In the case of  $C_2H_2$ -DME mixtures, NO decreases of approximately 30% have been achieved (Fig. 4) only under oxidizing conditions and temperatures near 850 K, where the production of glyoxal (reaction (R.13)) seems to be important. The glyoxal produced decomposes to formyl radicals (reactions (R.14) and (R.15)), and subsequently produces  $HO_2$  (reaction (R.32)).



Moreover, under these conditions of high oxygen availability ( $\lambda = 20$ , and NO presence), DME is initially converted into  $CH_3OCH_2$  radicals through reaction (R.33), increasing the formation of  $HO_2$  radicals.



Reaction rate analyses indicate that NO is converted into  $NO_2$  by reaction with  $HO_2$  radicals (reaction (R.26)), but  $NO_2$  is recycled back to NO by reaction with hydrogen atoms (reaction (R.34)) and  $CH_3$  radicals (reaction (R.35)), so no net reduction of  $NO_x$  is achieved.



A first-order sensitivity analysis to the kinetic parameters included in the mechanism used for modeling calculations has been performed for selected experiments, both in the absence and presence of NO. The impact on the CO concentration has been evaluated. Table 2 shows the results obtained. The temperatures chosen for the analysis correspond to the initiation conditions of the conversion of the mixtures, i.e., when CO has reached a value of approximately 10 ppm.

The results obtained indicate that  $C_2H_2$  conversion in the presence of DME is sensitive to almost the same reactions as in the absence of this additive [22]. It is worth to note that only under fuel-lean conditions the reactions involving glyoxal ( $OCHCHO$ ) present a high sensitivity, and also the DME oxidation route through methoxymethyl-peroxy ( $CH_3OCH_2O_2$ ). Results are also sensitive to reactions involved in NO reduction, in particular to those that imply the competition between  $HCCO + NO$  and  $HCCO + O_2$ , and also  $CH_3 + NO_2$ .

## 5. Conclusions

A study of the conversion of  $C_2H_2$ -DME mixtures at atmospheric pressure, analyzing the influence of temperature, air excess ratio ( $\lambda$ ) and presence of NO has been performed under flow reactor conditions. The results obtained have been interpreted in terms of a detailed kinetic mechanism. An extensive discussion including a comparison of the results with the literature data of individual  $C_2H_2$  [22] and DME [27] oxidation, in the absence and presence of NO [23], has been made.

Unlike what observed in their individual behaviors, the onset temperature for the  $C_2H_2$  and DME conversion in the oxidation of their mixtures depends on the oxygen availability, being lower for the highest value of the air excess ratio considered ( $\lambda = 20$ ). The reaction pathways for  $C_2H_2$  conversion in the presence of DME are basically the same as those in its absence. In this way, the DME addition only modifies the radical pool, and it could act as an inhibitor or promoter in acetylene consumption depending on the oxygen availability and the amount of DME present in the mixture. For fuel-rich conditions, increasing the amount of DME in the mixture seems to have an inhibitory effect on  $C_2H_2$  consumption. When DME is present in the mixture, less H radicals participate in acetylene consumption through the H addition to form vinyl radicals, and as a consequence, acetylene conversion is shifted to higher temperatures. However, for fuel-lean conditions, the trend is the opposite, and the DME presence promotes  $C_2H_2$  conversion, probably due to the increasing of O and OH radical formation which is favored because of the fuel-leaner conditions. Therefore, both DME and  $C_2H_2$  conversions are shifted to lower temperatures.

Acetylene, DME and their intermediates may interact with NO, reaching different NO diminution levels depending on the conditions. The higher NO decrease levels were achieved in absence of DME for temperatures above 1100 K and fuel-rich ( $\lambda = 0.7$ ) and stoichiometric conditions ( $\lambda = 1$ ). This is due to the competition between reactions of HCCO with NO and with  $O_2$ . By increasing the oxygen availability, the  $HCCO + O_2$  reactions predominate reaching a lower NO decrease level. However, under fuel-lean conditions ( $\lambda = 20$ ), the presence of DME increases the NO diminution from 13 to 30% mainly due to  $CH_3$  radicals generated from its conversion, which can react with NO or  $NO_2$ .

In general, modeling predictions are in good agreement with the experimental data trends obtained for the conditions studied. The model is able to reproduce the main experimental trends for  $C_2H_2$ , DME, CO,  $CO_2$ , and NO concentrations. However, it only includes gas-phase reactions and improvements are still needed, especially in reactions related to acetylene conversion, where higher discrepancies have been observed.

## Acknowledgements

The authors express their gratitude to Aragón Government and European Social Fund (GPT group), and to MINECO and FEDER (Project CTQ2015-65226) for financial support. Ms. Marrodán acknowledges Aragón Government for the predoctoral grant awarded.

## Appendix A. Supplementary material

Supplementary data associated with this article can be found, in the online version, at <http://dx.doi.org/10.1016/j.fuel.2016.06.011>.

## References

- [1] Yanfeng G, Shenghua L, Hejun G, Tiegang H, Longbao Z. A new diesel oxygenate additive and its effects on engine combustion and emissions. *Appl Therm Eng* 2007;27:202–7.
- [2] Tran LS, Sirjean B, Glaude P, Fournet R, Battin-Leclerc F. Progress in detailed kinetic modeling of the combustion of oxygenated components of biofuels. *Energy* 2012;43:4–18.
- [3] Tutak W, Lukács K, Szwaja S, Bereczky Á. Alcohol-diesel fuel combustion in the compression ignition engine. *Fuel* 2015;154:196–206.
- [4] Crookes RJ, Bob-Manuel KD. RME or DME: a preferred alternative fuel option for future diesel engine operation. *Energy Convers Manage* 2007;48:2971–7.
- [5] Verbeek R, Van der Weide J. Global assessment of dimethyl-ether: comparison with other fuels. *SAE Tech. Pap.* 1997; 971607.
- [6] Arcoumanis C, Bae C, Crookes R, Kinoshita E. Synergistic effect of mixing dimethyl ether with methane, ethane, propane, and ethylene fuels on polycyclic aromatic hydrocarbon and soot formation. *Fuel* 2008;87:1014–30.
- [7] Abián M, Esarte C, Millera A, Bilbao R, Alzueta MU. Oxidation of acetylene-ethanol mixtures and their interaction with NO. *Energy Fuels* 2008;22:3814–23.
- [8] Härtl M, Seidenspinner P, Jacob E, Wachtmeister G. Oxygenate screening on a heavy-duty diesel engine and emission characteristics of highly oxygenated oxymethylene ether fuel OME<sub>1</sub>. *Fuel* 2015;153:328–35.
- [9] Song KH, Nag P, Litzinger TA, Haworth DC. Effects of oxygenated additives on aromatics species in fuel-rich, premixed ethane combustion: a modeling study. *Combust Flame* 2003;135:341–9.
- [10] Glassman I, Yetter RA. *Combustion*. 4th ed. Burlington: Academic Press; 2008.
- [11] Ruiz MP, Guzmán de Villoria R, Millera A, Alzueta MU, Bilbao R. Influence of different operation conditions on soot formation from  $C_2H_2$  pyrolysis. *Ind Eng Chem Res* 2007;46:7550–60.
- [12] Mendiara T, Domene MP, Millera A, Bilbao R, Alzueta MU. An experimental study of the soot formed in the pyrolysis of acetylene. *J Anal Appl Pyrolysis* 2005;74:486–93.
- [13] Saggese C, Sánchez NE, Frassoldati A, Cuoci A, Faravelli T, Alzueta MU, et al. Kinetic modeling study of polycyclic aromatic hydrocarbons and soot formation in acetylene pyrolysis. *Energy Fuels* 2014;28:1489–501.
- [14] Frenklach M. Reaction mechanism of soot formation in flames. *Phys Chem Chem Phys* 2002;4:2028–37.
- [15] Omidvarborna H, Kumar A, Kim DS. Recent studies on soot modeling for diesel combustion. *Renew Sust Energy Rev* 2015;48:635–47.
- [16] Esarte C, Callejas A, Millera A, Bilbao R, Alzueta MU. Influence of the concentration of ethanol and the interaction of compounds in the pyrolysis of acetylene and ethanol mixtures. *Fuel* 2011;90:844–9.
- [17] Esarte C, Millera A, Bilbao R, Alzueta MU. Effect of ethanol, dimethylether, and oxygen, when mixed with acetylene, on the formation of soot and gas products. *Ind Eng Chem Res* 2010;49:6772–9.
- [18] Bo Z, Weibiao F, Jingsong G. Study of fuel consumption when introducing DME or ethanol into diesel engine. *Fuel* 2006;85:778–82.
- [19] Ying W, Longbao Z, Hewu W. Diesel emission improvements by the use of oxygenated DME/diesel blend fuels. *Atmos Environ* 2006;40:2313–20.
- [20] Alzueta MU, Glarborg P, Dam-Johansen K. Low temperature interactions between hydrocarbons and nitric oxide: an experimental study. *Combust Flame* 1997;109:25–36.
- [21] Kristensen PG, Glarborg P, Dam-Johansen K. Nitrogen chemistry during burnout in fuel-staged combustion. *Combust Flame* 1996;107:211–22.
- [22] Alzueta MU, Borruey M, Callejas A, Millera A, Bilbao R. An experimental and modeling study of the oxidation of acetylene in a flow reactor. *Combust Flame* 2008;152:377–86.
- [23] Abián M, Silva SL, Millera A, Bilbao R, Alzueta MU. Effect of operating conditions on NO reduction by acetylene-ethanol mixtures. *Fuel Process Technol* 2010;91:1204–11.
- [24] Glarborg P, Alzueta MU, Dam-Johansen K, Miller JA. Kinetic modeling of hydrocarbon/nitric oxide interactions in a flow reactor. *Combust Flame* 1998;115:1–27.
- [25] Glarborg P, Alzueta MU, Kjærsgaard K, Dam-Johansen K. Oxidation of formaldehyde and its interaction with nitric oxide in a flow reactor. *Combust Flame* 2003;132:629–38.
- [26] Alzueta MU, Hernández JM. Ethanol oxidation and its interaction with nitric oxide. *Energy Fuels* 2002;16:166–71.
- [27] Alzueta MU, Muro J, Bilbao R, Glarborg P. Oxidation of dimethyl ether and its interaction with nitrogen oxides. *Isr J Chem* 1999;39:73–86.
- [28] Faßheber N, Friedrichs G, Marshall P, Glarborg P. Glyoxal oxidation mechanism: implications for the reactions  $HCO + O_2$  and  $OCHCHO + HO_2$ . *J Phys Chem A* 2015;119:7305–15.
- [29] Lutz AE, Kee RJ, Miller JA. Senkin: A fortran program for predicting homogeneous gas phase chemical kinetics with sensitivity analysis. Sandia Natl Lab Rep. SAND87-8248; 1988.
- [30] Kee RJ, Rupley FM, Miller JA. Chemkin-II: A fortran chemical kinetics package for the analysis of gas-phase chemical kinetics. Sandia Lab Rep. SAND87-8215; 1991.
- [31] Cipolat D. Analysis of energy release and  $NO_x$  emissions of a CI engine fueled on diesel and DME. *Appl Therm Eng* 2007;27:2095–103.
- [32] Park SH, Yoon SH. Injection strategy for simultaneous reduction of  $NO_x$  and soot emissions using two-stage injection in DME fueled engine. *Appl Energy* 2015;143:262–70.
- [33] Bilbao R, Millera A, Alzueta MU. Influence of the temperature and oxygen concentration on  $NO_x$  reduction in the natural gas reburning process. *Ind Eng Chem Res* 1994;33:2846–52.
- [34] Miller JA, Klippenstein SJ, Glarborg P. A kinetic issue in reburning: the fate of HCNO. *Combust Flame* 2003;135:357–62.
- [35] Faravelli T, Frassoldati A, Ranzi E. Kinetic modeling of the interactions between NO and hydrocarbons in the oxidation of hydrocarbons at low temperatures. *Combust Flame* 2003;132:188–207.
- [36] Dagaut P, Nicolle A. Experimental study and detailed kinetic modeling of the effect of exhaust gas on fuel combustion: mutual sensitization of the oxidation of nitric oxide and methane over extended temperature and pressure ranges. *Combust Flame* 2005;140:161–71.
- [37] Taylor PH, Cheng L, Dellinger B. The influence of nitric oxide on the oxidation of methanol and ethanol. *Combust Flame* 1998;115:561–7.
- [38] Marrodán L, Royo E, Millera A, Bilbao R, Alzueta MU. High pressure oxidation of dimethoxymethane. *Energy Fuels* 2015;29:3507–17.